PACS numbers: 42.55.Px; 85.30.Vw; 42.60.Mi
DOI: 10.1070/QE2000v030n04ABEH001721

Experimental study of the α-factor in InGaAs/AlGaAs/GaAs strained quantum-well lasers

A P Bogatov, A E Boltaseva, A E Drakin, M A Belkin, V P Konyaev

Abstract. A technique to determine experimentally the amplitude – phase coupling factor (α factor) in semiconductor laser diodes is proposed. The factor was obtained for InGaAs/AlGaAs/GaAs single-quantum-well lasers with injected-carrier concentrations from 1.5×10^{18} to 6×10^{18} cm^{-3}. It is shown that the α factor for such structures at the maximum of mode gain lies in the range 2 – 9, and its value for one and the same structure may differ severalfold, depending on the operating point of a laser.

1. Introduction

The so-called amplitude – phase coupling factor (or the α factor), which characterises the relation between changes in refractive index and gain with increasing carrier concentration in an active medium, is of considerable importance in the theory of semiconductor lasers. This factor has an effect on a number of laser radiation characteristics of primary importance, which accounts for the interest in its measurement and calculation during the past decade [1 – 16]. In particular, the α factor is one of the main parameters determining the spectral line width of semiconductor lasers [1 – 4] (it is also called the line broadening factor). The α factor is expressed by the ratio of the rates of changes in effective refractive index and mode gain caused by changes in carrier concentration:

$$\alpha = -\frac{4\pi}{\lambda}\,\frac{\mathrm{d}n/\mathrm{d}N}{\mathrm{d}G/\mathrm{d}N}\,,$$

where λ is the wavelength in vacuum; n is the effective refractive index; G is the mode gain, and N is the injected-carrier concentration. The decrease of the α factor is noteworthy, because this allows us to develop structures with improved dynamic and noise characteristics of laser radiation.

Theoretical calculations of the α factor [14 – 16] and its experimental study in new types of laser structures [5, 6, 10 – 13] are particularly interesting. In Ref. [13] values of α in the range 2.2 – 3.5 for InGaAs quantum-well lasers were reported. However, the dependence of this parameter on the carrier concentration was not presented there. In this paper we report our results of the experimental determination of the α factor for InGaAs/GaAs strained quantum-well lasers. They were obtained by studying their superluminescence emission under threshold conditions. Such studies allow a simultaneous measurement of changes in the effective refractive index and mode gain caused by changes in pump current. They give information on the concentration dependence of the α factor in the lasers under study.

2. Experiment

The α factor was measured in InGaAs/AlGaAs/GaAs strained single-quantum-well lasers emitting radiation in the range 0.94 – 0.98 μm. The thicknesses and the composition of the layers comprising the structure are presented in Table 1.

The value of the optical confinement parameter calculated for the given structure is $\Gamma \approx 0.017$. In the calculation, we used for all layers, except the active one, the refractive indices obtained by the interpolation from the data in Ref. [17]. The refractive index of the active layer was equal to 3.63 [18]. The diode mirrors had no reflecting coatings. The samples studied by us represented laser diodes with a ridge waveguide (the ridge was 3.5 μm wide). They were fabricated from one heterostructure but had different cavity lengths (200, 400, and 600 μm). The diodes had threshold currents in the range of 13 – 15 mA, and the external differential efficiency (from both mirrors) was 0.6 – 0.8 W A^{-1}.

The spectra of amplified spontaneous emission were measured on a computerised setup on the basis of a multichannel optical spectrum analyser (Fig. 1). The diode emission was projected by two microobjectives onto the entrance slit of a DFS-24 spectrometer. A slit aperture place between the microobjectives was oriented perpendicular to the structure layers and separated out the fundamental

Table 1. Parameters of the heterostructure being studied.

Layer	Composition	Thickness/nm
Contact	p^+-GaAs	200
Emitter	P-$Al_{0.33}Ga_{0.67}As$	1.3×10^3
Waveguide	$Al_{0.23}Ga_{0.77}As$ undoped	90
Separating	GaAs undoped	6
Active	$In_{0.20}Ga_{0.80}As$	10
Separating	GaAs undoped	6
Waveguide	$Al_{0.23}Ga_{0.77}As$ undoped	90
Emitter	N-$Al_{0.33}Ga_{0.67}As$	1.6×10^3
Substrate	n-GaAs	10^5

A P Bogatov, A E Drakin P N Lebedev Physics Institute, Russian Academy of Sciences, Leninskiĭ prospekt 53, Moscow, 117924 Russia;
A E Boltaseva, M A Belkin Moscow Institute (State University) of Physics and Engineering, Dolgoprudnyĭ, Moscow oblast, 141700 Russia;
V P Konyaev 'Polyus' Research Institute, Federal State Enterprise, ul. Vvedenskogo 3, 117342 Moscow, Russia

Received 28 October1999
Kvantovaya Elektronika **30** (4) 315 – 320 (2000)
Translated by A N Kirkin; edited by M N Sapozhnikov

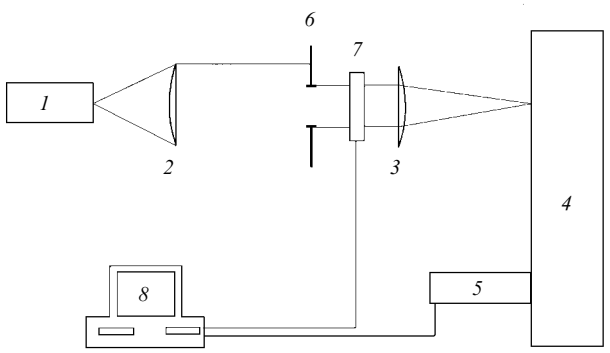

Figure 1. Schematic diagram of the experimental setup: (1) laser diode, (2, 3) focusing microobjectives, (4) DFS-24 spectrometer, (5) photodiode array, (6) slit aperture, (7) shutter, (8) computer.

transverse mode of laser emission. A photodiode array placed in the plane of the exit monochromator slit consisted of 1024 elements with a period of 25 μm.

The dynamic range of the system in measuring the intensity was $\sim 1.6 \times 10^3$. The data from the diode array were transferred to a computer. A computer-controlled shutter placed in front of the focusing objective let us determine the dark current of the diode array and the background emission when recording each spectrum. To decrease noise, the diode array was cooled down to -25 °C. The spectra were measured at a constant temperature (18 °C) of a copper laser holder. The temperature was controlled by the current traversing a Peltier element or a heater.

The measurements were carried out under continuous pumping conditions. For each diode we recorded series of spectra with a current step of 1 mA. The step was chosen from the condition that the mode shift caused by this change should be much smaller than the intermode interval, which made it possible to determine the shift of each mode. In a wavelength region near 1 μm, the diode array covered a spectral range of width ~ 20 nm. The spectral range studied in the experiments was 130 nm wide. When measuring spectra, we divided these into 9 overlapping subbands ~ 20 nm wide (9 fixed positions of spectrometer gratings). To join the spectra we determined the shifts of concrete modes when making a change from one subband to another.

The mode shift obtained on changing the pump current was caused not only by a change in injected-carrier concentration, but also by a temperature change due to the power released in a diode. Because of this, for each diode we recorded several spectra above the lasing threshold, which allowed us estimate the temperature contribution to the change in refractive index.

Thus the initial data for mathematical processing represented digitised superluminescence spectra for different pump currents (for each diode, 12 to 14 spectra below the threshold and 5 to 6 spectra above the threshold). In a particular case of the diode with the cavity length $L = 600$ μm, they contained up to 480 modes.

3. Method of spectrum processing

In experimentally determining the α factor, we processed the superluminescence spectra of laser diodes, i.e., the spectra of amplified spontaneous emission of a laser operating below the threshold. We used a favourable property of a semiconductor laser, namely, the fact that the spontaneous emission from its active region is sufficiently high for experimental detection. It can be used as the probing radiation entering a laser cavity. If the transverse field structure is described by the single fundamental mode, this cavity may be treated as a Fabry–Perot cavity. The spectrum of spontaneous emission will be modulated by longitudinal resonances of the cavity.

Note that there exists a direct analogy between the classical transmission spectrum of a Fabry–Perot cavity and the spectra of the radiation inside this cavity and the radiation coupled out from it [19]. In both cases, we deal with the longitudinal resonances of a Fabry–Perot cavity. The waveguide character of the propagation of radiation between the cavity mirrors, which is typical of a semiconductor laser, leads to a certain distinction of this cavity from the classical Fabry–Perot cavity.

This distinction consists in the fact that the refractive index of a homogeneous medium filling the classical cavity is replaced with the effective refractive index of the mode under consideration $n = \beta'/k_0$, where β' is the real part of the complex constant of waveguide propagation $\beta = \beta' + \mathrm{i}\beta''$; $k_0 = \omega/c$ is the wave number in vacuum. In what follows, we assume that the dependence of the electromagnetic-wave amplitude on the coordinate along the cavity axis and the time t is proportional to $\exp(\mathrm{i}\beta z - \mathrm{i}\omega t)$. Now the amplitude–phase coupling factor α can be also determined to be

$$\alpha = \left(\frac{\partial\beta'}{\partial N}\right)\left(\frac{\partial\beta''}{\partial N}\right)^{-1} .$$

One can use the transmission line of a cavity or the ratio of intensities at a minimum and a maximum to determine the cavity parameters, in particular, the mirror reflectivities and absorption (gain) in a cavity. This is the basis of a number of methods used for measuring the dependence of gain on the pump current in a semiconductor laser [20–22].

To determine a change in refractive index with pump current we found for each experimental spectrum an exact position of maxima of the cavity. For this purpose, we used numerical fitting of the theoretical model to the experimental spectra by the least-squares method. Each spectral peak was described by the Airy function

$$I_k(\lambda) = \frac{A_k(1)}{A_k(2) - \cos[A_k(3)(A_k(4) - \lambda)]} , \qquad (1)$$

where λ is the wavelength. We fitted the coefficients $A_k(p)$, $p = 1 - 4$.

Fig. 2 presents a fragment of the superluminescence spectrum of the diode with the cavity length $L = 600$ μm for the pump current $i = 10$ mA (squares). The solid curve represents the model function (1) with the coefficients determined by the fitting procedure carried out for the central peak in Fig. 2. Thus a set of these coefficients determined fully the position of the maximum of each longitudinal mode. From the shift of superluminescence modes caused by the change in the pump current, we determined the change in the effective refractive index.

It is known that the change in the effective refractive index changes with pump current i is due to the changes in injected-carrier concentration N and diode temperature T:

$$\frac{\mathrm{d}n}{\mathrm{d}i} = \frac{\partial n}{\partial N}\frac{\partial N}{\partial i} + \frac{\partial n}{\partial T}\frac{\partial T}{\partial i} . \qquad (2)$$

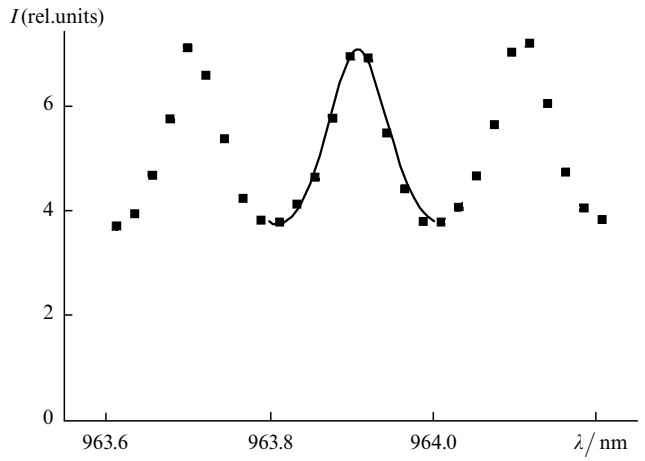

Figure 2. Fragment of the superluminescence spectrum of the diode with the cavity length $L = 600$ μm for a pump current of 10 mA (■) and the model function of superluminescence described by formula (1) (solid curve).

It is favourable that the temperature and concentration changes of n have different signs. Because of this, one can easily separate these effects. Indeed, above the lasing threshold, the carrier concentration is stabilised, Δn is determined only by heating and depends linearly on the pump current. From the slope of the curve $\Delta n = f(i)$ above the lasing threshold, one can determine the temperature contribution to the change in refractive index both above the lasing threshold and below it.

Assuming that all the input power below the lasing threshold is spent on diode heating, we obtain $(\partial T/\partial i)|_{\rm sp} = RU$, where R is the thermal resistance of a diode, and U is the voltage across a diode. Above the lasing threshold, a portion of power emerges from a diode in the form of radiation. Because of this, $(\partial T/\partial i)|_{\rm las} = R(U - \eta)$, where η is the external differential efficiency from both mirrors (in $\mathrm{W\,A^{-1}}$). As a result, the relation between the derivatives $\partial T/\partial i$ below the lasing threshold and above it is determined by the expression

$$\left(\frac{\partial T}{\partial i}\right)\Big|_{\rm sp} = \frac{U}{U-\eta}\left(\frac{\partial T}{\partial i}\right)\Big|_{\rm las} .$$

From this relation and expression (2) it follows that

$$\left(\frac{\partial n}{\partial N}\right)\left(\frac{\partial N}{\partial i}\right)\Big|_{\rm sp} = \frac{{\rm d}n}{{\rm d}i}\Big|_{\rm sp} - \frac{U}{U-\eta}\frac{{\rm d}n}{{\rm d}i}\Big|_{\rm las} . \qquad (3)$$

To determine the relation between the injected-carrier concentration N and the pump current i, the rate of change in refractive index with concentration $\partial n/\partial N$ was assumed to be constant in the range of pump currents considered and to be the same for all diodes. Assuming that the carrier concentration at small pump currents is directly proportional to the current density and that the carrier lifetime is known (1 ns), one can determine the dependence of the change in effective refractive index on the carrier concentration.

The method used most extensively to measure the mode gain is based on determining the modulation depth in the laser emission spectrum below the threshold (Hakki – Paoli method) [13, 20]. Its disadvantage is that the method requires high-resolution equipment and the presence of background radiation in the spectral interval between the Fabry – Perot resonances, which makes a large contribution to the measurement error.

There exist a number of modifications to this method, which allow us, to a certain extent, to take the effect of the spread function [21, 22] into account. In this work we used an original technique, which consists of expressing gain in terms of the interval between the Fabry – Perot resonances $\Delta\lambda$ and the resonance width $\delta\lambda_\beta$ at a certain intensity level β:

$$I_\beta = I_{\min} + \beta(I_{\max} - I_{\min}) , \quad 0 \leqslant \beta \leqslant 1 , \qquad (4)$$

where $I_{\max}$, $I_{\min}$ are the intensities at the maximum and minimum of a resonance peak. Assuming that the spectrum of amplified emission in the region of the mth resonance is described by the function

$$I(\lambda) = \frac{A}{[(1+F^2)/2F] - \cos[2\pi(\lambda_m - \lambda)/\Delta\lambda_m]} , \qquad (5)$$

where A is the amplitude; $\Delta\lambda_m = \lambda_m^2/2n^*L$ is the intermode distance; $F = \exp(GL); G = \Gamma g - \alpha - L^{-1}\ln R^{-1}$ is the coefficient of modal net gain; n^* is the group refractive index, and L is the diode length. One can obtain from equations (4) and (5) the relation between $\delta\lambda_\beta/\Delta\lambda_m$ and F:

$$\cos\left(\pi\frac{\delta\lambda_\beta}{\Delta\lambda_m}\right) = \frac{(1+F^2)(2\beta-1)+2F}{1+F^2+2F(2\beta-1)} . \qquad (6)$$

The lasing threshold is characterised by the condition $\delta\lambda_\beta = 0$. However, the mode width at a certain level β of the spectrum being recorded, i.e., $\delta\lambda_\beta^{\rm r}$, is somewhat larger than $\delta\lambda_\beta$ because of the broadening caused by the spread function.

We took the spread function into account in the following way. We assumed that β close to unity was characterised by the approximate equality

$$\left(\delta\lambda_\beta^{\rm r}\right)^2 \approx \left(\delta\lambda_\beta\right)^2 + \left(\delta\lambda_\beta^{\rm a}\right)^2 , \qquad (7)$$

where $\delta\lambda_\beta^{\rm a}$ is the width of the spread function at the level β. Expression (7) is valid because the spectral curves and the spread function near a maximum can be approximately described by the Gaussian curves [for the latter, expression (7) is fulfilled exactly]. As a result, we have at the lasing threshold

$$\delta\lambda_\beta^{\rm r} \approx \delta\lambda_\beta^{\rm a} . \qquad (8)$$

First, we determined with the aid of expression (6) the curves of mode gain taking no account of the spread function. After that we estimated the width of the spread function at the level $\beta = 0.8$ for the threshold current, when the laser spectral line is known to be considerably narrower than the spread function. In our experiments this width was 0.011 nm, which corresponds to the spectral resolution by Rayleigh criterion at a level of 0.03 nm. After that we found the true width of each mode for all spectra with expression (7).

4. Results and discussion

A typical experimental dependence of changes in effective refractive index with pump current density j at the wavelength $\lambda_0 = 984.83$ nm, which was obtained for the diode with the cavity 400 μm long (with threshold current

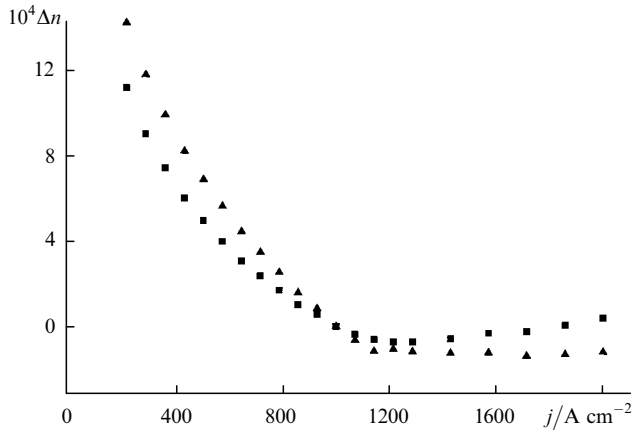

Figure 3. Dependences of the change in effective refractive index on the pump current measured experimentally (■) and corrected for the temperature component (▲) for the diode with cavity length $L = 400$ μm and the wavelength $\lambda_0 = 984.83$ nm ($j_0 = 1000$ A cm^{-2}).

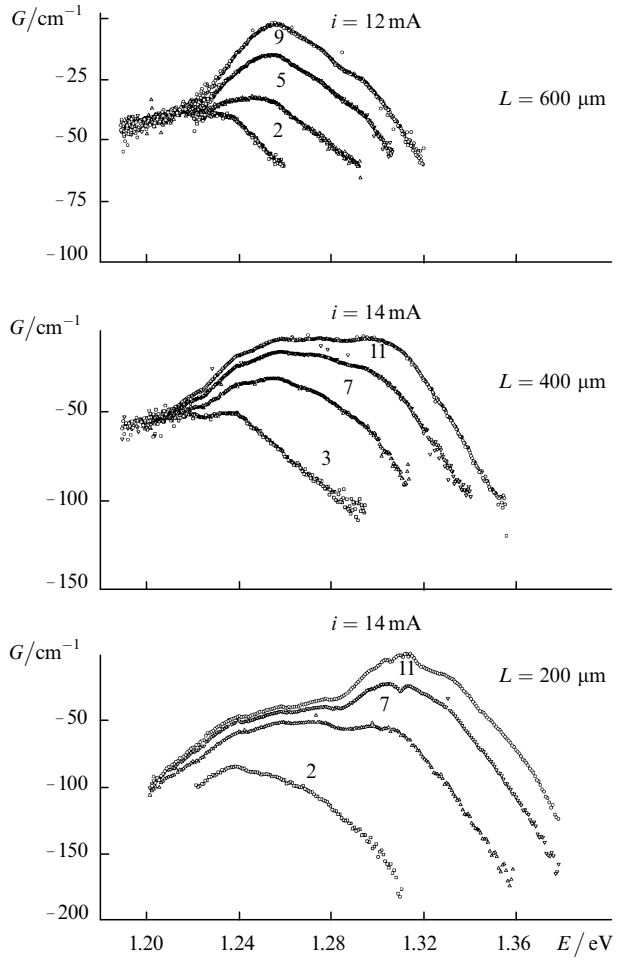

Figure 4. Spectral dependences of the mode gain G for three diodes with cavity lengths of 600, 400, and 200 μm for different pump currents.

$i_0 = 14$ mA and current density $j_0 \approx 1000$ A cm^{-2}), is presented in Fig. 3 (squares). The dependence $\Delta n(j)$, corrected for the temperature component $\partial n/\partial T$ according to the method described above, is presented in the same figure (triangles). One can see that the initial curve is characterised by a decrease in $n[\Delta n = n(j) - n(j_0)]$ up to the current density $j \approx 1100$ A cm^{-2}, which is associated with the action of carriers, and a further increase in j manifests the temperature dependence of the effective refractive index, and n increases in this region.

The experimental dependences of mode gain on photon energy E are shown in Fig. 4. We present some of the experimental curves, which are corrected for the width of the spread function, for three diodes with $L = 600$, 400, and 200 μm and different pump currents. The gain was found to increase as the cavity length decreased, which is associated with the optical transitions from the second quantum level to which correspond a photon energy of about 1.31 eV. For the diode with $L = 200$ μm, one can clearly see the saturation of gain for the transitions from the first level; to these transitions corresponds a photon energy of about 1.26 eV.

Using the experimental data on the change in effective refractive index and the mode gain, we calculated the α factor for the studied samples. The resulting dependences of the α factor at the maximum of mode gain on the injected-carrier concentration for the diodes are presented in Fig. 5. When the injected-carrier concentration N changed from 1.5×10^{18} to 6×10^{18} cm^{-3}, the α factor for three diodes with $L = 200$, 400, and 600 μm was found in the range 2 – 9, which agrees with the previously published data (in Ref. [14], where N was changed from 2×10^{18} to 6×10^{18} cm^{-3}, the α factor was found in the range 2.5 – 6).

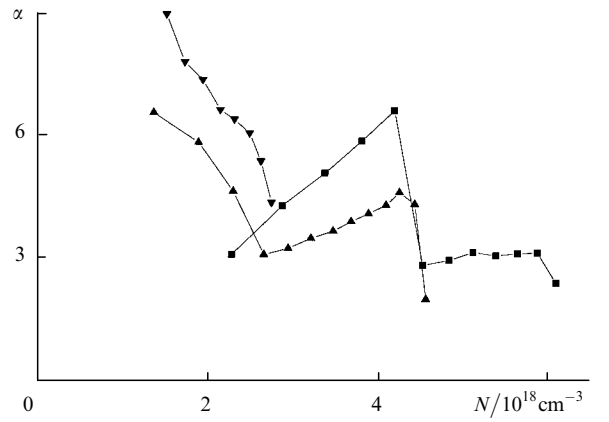

Figure 5. Dependences of the α-factor at the maximum of mode gain on the injected-carrier concentration for the diodes with cavity lengths of 200 (■), 400 (▲), and 600 μm (▼).

For each diode, the behaviour of the α factor is largely regular. It decreases with increasing concentration N up to $(2-2.5)\times10^{18}$ cm^{-3}, which is associated with an increase in differential gain in this range for the transitions from the first level. As N is increased further up to $(4-4.5)\times10^{18}$ cm^{-3}, the α factor increases gradually because of the saturation of gain for the transitions from this level. At $N = (4-4.5)\times10^{18}$ cm^{-3}, it decreases sharply, which is related to the fact that the gain maximum changes to the transitions from the second level (Fig. 4), and, as the concentration is increased further, one again observes a gradual increase in the α factor.

The dependence of the α factor on the carrier concentration N for three fixed photon energies is presented in Fig. 6. One can see that the α factor predominantly shows a monotonic increase with increasing N, which is associated

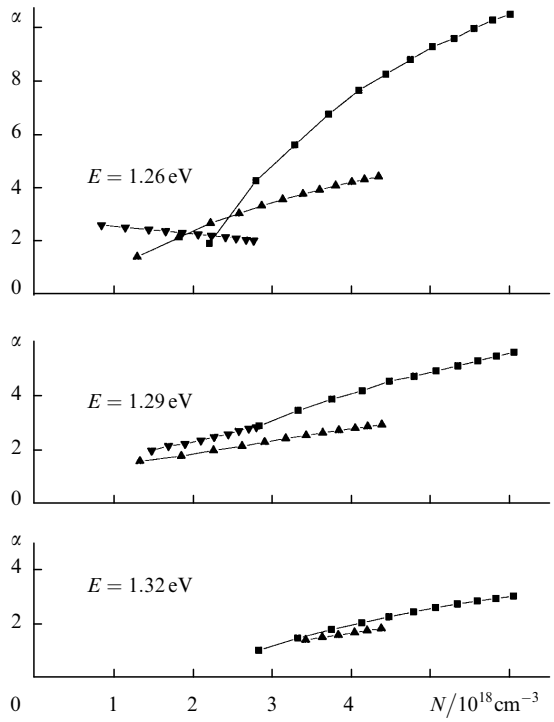

Figure 6. Dependences of the α-factor on the injected-carrier concentration for fixed photon energies of 1.26, 1.29, and 1.32 eV for cavity lengths of 200 (■), 400 (▲), and 600 μm (▼).

with an inevitable saturation of material gain at a fixed wavelength.

The spread of experimental values is not associated with the measurement error, but is caused by the actual behaviour of α. The error of determining α by the method described above is estimated to be not worse than ±5%. One should bear in mind, first, that α is determined by the ratio of derivatives and therefore has a higher sensitivity to the change in carrier concentration than the initial quantities, such as the refractive index or gain. Second, because α was found for the wavelength corresponding to the spectral maximum, which, in turn, is characterised by a rather complex, although monotonic, change with increasing concentration, α changes in a rather complex way and, in particular, undergoes sharp changes.

It is clear from the above discussion that α can change severalfold depending on the operating point of a laser, namely, on the threshold electron concentration. The threshold concentration (threshold gain), in turn, depends on such laser parameters as the cavity length, the optical confinement factor, the mirror reflectivities, and the nonresonant intracavity loss. It is evident that changes in these parameters cause a change in the α factor.

Because the α factor depends greatly on the concentration, one should take the spatially nonuniform depletion of inversion along the axis of a laser diode cavity into account when analysing the physical phenomena in which this factor is important, specifically, when analysing the laser line width [4]. This effect is most pronounced in lasers operating at high pump currents (considerably exceeding the threshold value) and lasers having a mirror with a low reflectivity.

Note that we obtained different values of the α factor for the same carrier concentration but different diodes, which is likely to be associated with its dependence on characteristics of a concrete sample. The diodes with cavities of different length studied by us were fabricated from the same sample of a heterostructure, although their internal parameters (layer thickness, ridge structure, current spreading, etc.) might be somewhat different because of inevitable technological nonuniformities in the course of structure production.

From our measurements it also follows that the value of the α factor itself and its dependence on the concentration in a semiconductor laser with a spectrally nonselective plane cavity and a laser with a spectrally selective cavity (in particular, in a laser with distributed feedback) will be radically different. In the latter, the α factor may be considerably larger than in a conventional laser with plane-parallel mirrors.

5. Conclusion

Thus the α factor in the laser structure studied by us can change from 2 to 9 depending on the threshold carrier concentration (which is determined, in particular, by the cavity length, the mirror reflectivities, etc.); i.e., it is not constant. Therefore the α factors in lasers with uncontrollable laser parameters may be substantially different.

Because a decrease in the α factor stabilises the emission spectrum and improves dynamic and laser noise characteristics, one can use our results to choose the laser operating conditions corresponding to the optimum range of the α factor. In particular, in the case where small α is required, a low threshold concentration (threshold material gain) may be unsuitable.

Acknowledgements. This work was supported by the 'Physics of Solid-State Structures' Program and the 'Integration' Federal Dedicated Program ('Fundamental Optoelectronics of Quantum-Well Semiconductor Structures' and 'Fundamental Optics and Spectroscopy' Educational and Scientific Centres).

References

1. Henry H IEEE J. Quantum Electron. **18** 259 (1982)
2. Vahala K, Yariv A IEEE J. Quatum Electron. **19** 1096 (1983)
3. Vahala K, Chiu L C, Margalit S, Yariv A Appl. Phys. Lett. **42** 631 (1983)
4. Wu M-C, Lo Y, Wang S Appl. Phys. Lett. **52** 1119 (1988)
5. Dutta N K, Wynn J, Sivco D L, Cho A Y Appl. Phys. Lett. **56** 2293 (1990)
6. Dutta N K, Temkin H, Tanbun-Ek T, Logan R Appl. Phys. Lett. **57** 1390 (1990)
7. Grabmaier A, Fuchs G, Hangleiter A J. Appl. Phys. **70** 2467 (1991)
8. Zhao B, Chen T R, Iannelli J, Zhuang Y H, Yamada Y, Yariv A Appl. Phys. Lett. **62** 1200 (1992)
9. Hamel W A, van Exter M P, Shore K A, Woerdman J P Phys. Rev. **45** 4864 (1992)
10. Raghuraman R, Yu N, Engelmann R, Lee H, Shieh C L IEEE J. Quantum Electron. **29** 69 (1993)
11. Kikuchi K, Amano M, Zah C E, Lee T P IEEE J. Quantum Electron. **30** 571 (1994)
12. Danilina O V, Logginov A S, Kvantovaya Elektron. (Moscow) **22** 1079 (1995) [Quantum Electron. **25** 1043 (1995)]
13. Konyaev V P, Kurnosov V D, Luk'yanov V N, Plyavenek A G, Shramenko M V, Yakubovich S D Kvantovaya Elektron. (Moscow) **21** 1137 (1994) [Quantum Electron. **24** 1054 (1994)]
14. Hader J, Bosset D, Stohs J, Chow W W, Koch S W, Moloney J W Appl. Phys. Lett. **74** 2277 (1999)
15. Anson S A, Olesberg J T, Flatte M E, Hasenberg T C, Boggess T F J. Appl. Phys. **86** 713 (1999)

16. Wenzel H, Erbert G, Enders P M IEEE J. Sel. Top. Quantum Electron. **5** 637 (1999)
17. Gasey N C, Jr., Panis M B Heterostructure Lasers (New York: Academic Press, 1978)
18. Zou W X, Merz J L, Coldren L A J. Appl. Phys. **72** 5047 (1992)
19. Bezotosnyĭ V V, Bogatov A P, Dolginov L M, Drakin A E, Eliseev P G, Mil'vidskiĭ M G, Sverdlov B N, Shevchenko E G Trudy FIAN **141** 3 (1983)
20. Paoli T, Hakki B J. Appl. Phys. **44** 4113 (1973)
21. Cassidy D T J. Appl. Phys. **56** 3096 (1984)
22. Westbrook L D Proc. IEEE **133** 135 (1986)